Automatic Nuchal Translucency Measurement from Ultrasonography

JinHyeong Park[1], Michal Sofka[1], SunMi Lee[2], DaeYoung Kim[2], and S. Kevin Zhou[1]

[1] ICV TF, Siemens Corporation, Corporate Technology, Princeton, NJ 08540 USA
[2] H CP US PLM, Siemens Limited Seoul, Bundang Seongnam, Gyeonggi, Korea

Abstract. This paper proposes a fully automatic approach for computing Nuchal Translucency (NT) measurement in an ultrasound scans of the mid-sagittal plane of a fetal head. This is an improvement upon current NT measurement methods which require manual placement of NT measurement points or user-guidance in semi-automatic segmentation of the NT region. The algorithm starts by finding the pose of the fetal head using discriminative learning-based detectors. The fetal head serves as a robust anchoring structure and the NT region is estimated from the statistical relationship between the fetal head and the NT region. Next, the pose of the NT region is locally refined and its inner and outer edge approximately determined via Dijkstra's shortest path applied on the edge-enhanced image. Finally, these two region edges are used to define foreground and background seeds for accurate graph cut segmentation. The NT measurement is computed from the segmented region. Experiments show that the algorithm efficiently and effectively detects the NT region and provides accurate NT measurement which suggests suitability for clinical use.

1 Introduction

Nuchal Translucency (NT) refers to the fluid-filled region under the skin of posterior neck of a fetus. Increased NT in early gestation period is correlated to the high risk of major cardiac defects and chromosomal defection including Down Syndrome [1]. The NT screening is performed in the first trimester of pregnancy using ultrasound scans. A sonographer first needs to navigate to the mid-sagittal plane containing echogenic nasal tip along with nasal bone, and translucent diencephalon in the center (Fig. 1). The plane is then stored and the measurement computed from manually placed marks. The accuracy requirement on the measurement is very high since even a slight deviation can completely change the diagnosis [1]. This makes the manual measurement and the design of automated tools difficult.

There have been semi-automatic approaches [2,3] to detect the NT measurement in 2D scans of mid-sagittal plane. In these approaches, the user is required to manually specify a region-of-interest (ROI) surrounding the NT measurement location. The ROI is used as input to the segmentation algorithm for finding upper and lower edges of the NT region. The final NT thickness is computed from

K. Mori et al. (Eds.): MICCAI 2013, Part III, LNCS 8151, pp. 243–250, 2013.

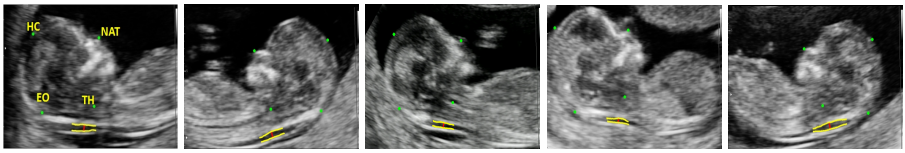

Fig. 1. Fetal ultrasound scans for measuring Nuchal Translucency (NT) in the mid-sagittal plane. NT (yellow lines) is a small fluid-filled region behind fetus neck. The NT detection is constrained by automatically found anchoring structure, fetal head, defined by stable landmarks (green): head crown (HC), throat (TH), nasal tip (NAT), and external occipital region (EO). The NT measurement is shown in red.

the traced edges as the maximum distance between them. Similarly, measuring the NT in 3D images is also performed on the mid-saggital plane, but the plane must be first found from the acquired ultrasound volume [4].

This paper proposes a fully automatic solution for NT measurement in 2D ultrasound scans of a mid-sagittal plane. Fig. 1 depicts typical examples of NT images used for NT measurements. The algorithm first detects the fetal head by implicitly relying on the appearance of stable structures that characterize the mid-sagittal plane: echogenic nasal tip, nasal bone, and translucent diencephalon. The NT region is predicted based on a statistical model obtained from the relative poses of the fetal head and the NT region. Approximate edges of the NT region are then found using Dijkstra's shortest path algorithm with graph weights extracted from the intensity image [5]. The edges are used to define foreground and background seed points for accurate Graph Cut segmentation algorithm [6]. Finally, the NT measurement value is computed from the segmentation result at the location of maximum thickness. To the best of our knowledge, this work is the first to propose the fully automatic NT measurement.

The paper is organized as follows. Background literature is briefly reviewed in Section 2. Section 3 formulates the problem of estimating the NT region using fetal head as an anchoring structure. The segmentation algorithm for accurately finding the NT edges is discussed in Section 4. Experimental results are presented in Section 5. The paper is concluded in Section 6.

2 Background

As mentioned in Section 1, the previously proposed methods for NT measurement in 2D ultrasound scans require manual steps [2,3]. The early techniques for automatically detecting other fetal structures relied on filtering, morphological operators, and Hough transform [7]. These techniques tend to be slow and are typically designed for a specific anatomy which makes them difficult to generalize to new structures. Chalana et al. [8] describe a method for detecting the biparietal diameter and head circumference based on active contour model. The algorithm does not use the image appearance which is necessary to increase the robustness and accuracy. Carneiro et al. [9] proposed a system for detecting and

measuring several anatomies in 2D ultrasound images using the same underlying algorithm. The method learns to discriminate between the structures of interest and background via a Probabilistic Boosting Tree classifier [10]. The appearance variations and imaging artifacts are captured by a large annotated database of images. An efficient search technique makes the system run in under half second. However, the detected structures are large (e.g. fetal limbs, abdominal circumference, crown rump length) and constraints between the structures are not exploited. Deng et al. [11] proposed an algorithm to locate NT bounding box using hierarchical model constructed from three SVM-based detectors of NT, Head, and Body. The algorithm has several limitations. It uses very coarse scale range of only 7 levels and does not provide NT orientations. Therefore, it does not provide automatic NT measurements, but only axis-aligned NT bounding boxes.

3 Automatic Estimation of the NT Region

In this section, we formally discuss the overall approach to automatically find the NT region. Let θ denote the parameter of NT pose represented by its position (x, y), width w, height h, and orientation α, and $\mathcal{I}_\theta$ denote the observed image patch parametrized by θ. Similarly, let us define φ and $\mathcal{I}_\varphi$ for fetal head. The goal is to find the parameter of the best pose $\hat{\theta}$ as:

$$\hat{\theta} = \arg\max_{\theta} P(\theta|\mathcal{I}) = \arg\max_{\theta} \int_{\varphi} P(\theta, \varphi|\mathcal{I}_\theta, \mathcal{I}_\varphi) d\varphi. \tag{1}$$

The term $P(\theta, \varphi|\mathcal{I}_\theta, \mathcal{I}_\varphi)$ inside the integral in Eq. (1) can be reformulated as follows by applying the Bayesian rule:

$$P(\theta, \varphi|\mathcal{I}_\theta, \mathcal{I}_\varphi) = \frac{P(\mathcal{I}_\theta|\theta, \varphi, \mathcal{I}_\varphi) P(\theta, \varphi|\mathcal{I}_\varphi)}{P(\mathcal{I}_\theta|\mathcal{I}_\varphi)} = \frac{P(\mathcal{I}_\theta|\theta) P(\theta, \varphi|\mathcal{I}_\varphi)}{P(\mathcal{I}_\theta|\mathcal{I}_\varphi)}, \tag{2}$$

where $P(\mathcal{I}_\theta|\theta, \varphi, \mathcal{I}_\varphi)$ can be simplified to $P(\mathcal{I}_\theta|\theta)$ because $\mathcal{I}_\theta$ is only depended by θ. By substituting Eq. (2) into Eq. (1), we obtain the following objective function:

$$\begin{aligned} \hat{\theta} &= \arg\max_{\theta} \int_{\varphi} \frac{P(\mathcal{I}_\theta|\theta) P(\theta, \varphi|\mathcal{I}_\varphi)}{P(\mathcal{I}_\theta|\mathcal{I}_\varphi)} d\varphi \\ &\approx \arg\max_{\theta} P(\mathcal{I}_\theta|\theta) \int_{\varphi} P(\theta|\varphi, \mathcal{I}_\varphi) P(\varphi|\mathcal{I}_\varphi) d\varphi \\ &= \arg\max_{\theta} P(\mathcal{I}_\theta|\theta) \int_{\varphi} P(\theta|\varphi) P(\mathcal{I}_\varphi|\varphi) P(\varphi) d\varphi. \end{aligned} \tag{3}$$

The first term in Eq. (3), $P(\mathcal{I}_\theta|\theta)$, is the likelihood of $\mathcal{I}_\theta$ given θ, which is obtained from a discriminative classifier trained to detect presence or absence of the NT region. Similarly, the likelihood $P(\mathcal{I}_\varphi|\varphi)$ is obtained from a discriminative classifier for the fetal head. The term $P(\theta|\varphi)$ represents the transition probability

of θ from φ, which is learned in a nonparametric manner to capture the geometric relationship between the fetal head and NT regions. The term $P(\varphi)$ is the prior probability for fetal head that is set as uniform.

3.1 Detection of Fetal Head and Nuchal Translucency

The algorithm employs discriminative learning [10,12,13,14] to compute the likelihoods of observing the fetal head and NT region Eq. (3). Robustness of the system is achieved by exploiting spatial relationships and multi-resolution hierarchy using Hierarchical Detection Network (HDN) [15]. In our case, the pose of the NT region is predicted using the most reliable candidates (samples) of the fetal head pose detected by the fetal head detector which is trained using three resolution levels (0.4 mm, 0.2 mm and 0.1 mm). The NT region detector uses two resolution levels (0.2 mm and 0.1 mm). The final HDN network is shown in Fig. 2-(a).

The multi-resolution hierarchy, has the advantage that the complexity of the training and detection (and therefore the complexity of the classifiers) is reduced by distributing it into each level. Global structures are best detected at the coarse resolution and provide constraints for local detection at finer resolutions. This way, the search space for the local detection is reduced which increases robustness since many image regions are never considered. In addition, computational speed is increased due to the reduced search space.

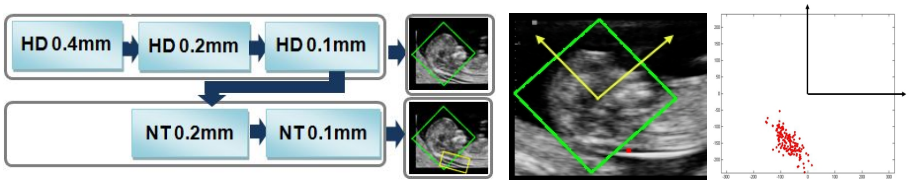

Fig. 2. (a) The hierarchy of the detectors. HD represents the fetal head detector and NT represents the NT region detector. 0.4 mm, 0.2 mm and 0.1 mm indicate the three image resolutions. (b) Fetal head bounding box (green) and NT location (red point). The two yellow axes define the local coordinate system based on the center and orientation of the fetal head. (c) The distribution of the NT location (red points) in the local coordinate system of the fetal head defined in (b). The black coordinate axes correspond to the yellow axes in (b).

It is clear that the successful detection of the NT region hinges on the modeling of the statistical relationship between the fetal head and the NT region. In this modeling, we rely on the strong anatomical prior present in the domain of fetal head scans. Fig. 2-(b) and (c) illustrate the statistical relationship between the NT position predicted from the pose of the head. For each image, the NT location is computed based on the local coordinate system defined by the head as

illustrated in Fig. 2-(b). The distribution of NT location in the local coordinate system is shown in Fig. 2-(d) where the origin is the location of the fetal head center. This distribution corresponds to $P(\theta|\varphi)$ in Eq. (3).

4 Nuchal Translucency Measurement

The NT measurement is computed from the segmentation of the NT region. The pose of the detected NT region is passed into the segmentation algorithm and the upper edge and the lower edge are initially segmented based on the directional gradient of the edge. The Dijkstras algorithm computes each path separately using two inversed gradient magnitude images which are generated by applying oriented gradient filters (rotated 180 degrees w.r.t. each other). Segmentation seeds are placed between the initial paths for foreground and outside of them for background. The seeds are used in a Graph Cut segmentation algorithm to find an accurate segmentation of the NT region. The NT measurement value is computed from as the maximum thickness of the NT region segmentation.

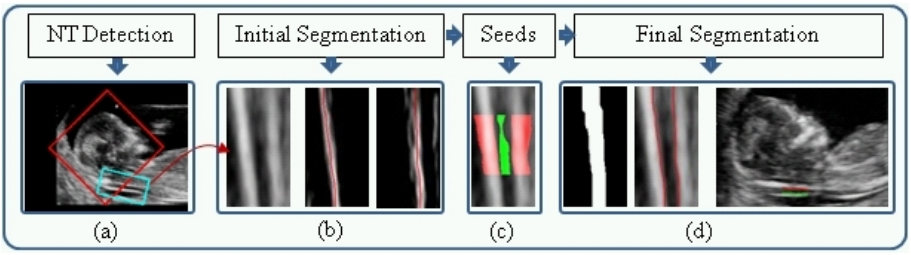

Fig. 3. Algorithm flow of NT segmentation using the NT region detection result. (a) The pose of the detected NT region is used for defining the segmentation region. (b) The initial NT region edges are obtained from Dijkstra's shortest path on the inverse gradient magnitude as the cost. (c) The NT edges are used to define foreground (green) and background (red) seeds. (d) The final segmentation is obtained by running Graph Cut segmentation.

5 Experiments

Our dataset consists of 196 DICOM scans from the first trimester screening exams. Experts annotated the fetal head and the NT region as shown in Fig. 1. The fetal head is annotated using 4 landmarks shown as green points in Fig. 1 and they are used to define the pose of the fetal head as follows. The two points on head crown and on throat define the orientation and the height of the bounding box, and the other two points on nasal tip and external occipital region define the width of the bounding box. The two yellow lines represent the NT edges and the red line across the two edges is the one for actual measurement of NT thickness. If there is insufficient and ambiguous information in an image for annotation, experts were encouraged to choose the best guess using the context of the image.

We normalized the orientation of fetal head such that the fetus always faces upwards and the head is towards the left side of the image. Standardizing the head pose helps to train more robust NT detector. During detection, the the head orientation is determined by using both the original input image and its left-to-right flipped image. The head orientation is decided based on the score of the two detection results. To achieve this, the detector is trained by generating images where the head is oriented towards the right side of the image and adding them to negative sample pool. Based on our experimental results, the algorithm can discriminate the head orientation in 100% of the cases. The images were resampled to 0.1 mm resolution. For performance evaluation, the collected data set was divided into two sets: randomly selected 80% for training and the remaining 20% for testing.

Our first experiment focuses on the robustness and accuracy of the fetal head and NT region detection. We use the following error metrics: angle difference (degree), center-to-center distance, and size difference, computed between the results from expert's ground truth and the algorithm. Table 1 shows the error between the ground truth and the algorithm detection of all the test data. The error of the NT location is slightly higher due to the inherent ambiguity in the accurate localization along the NT region. Overall, the detected NT region can be reliably used for the segmentation.

Table 1. Performance evaluation of the testing data. The angle difference is in degrees. The center and size errors are in millimeters.

Test Data (39)								
	Fetal Head				NT			
	mean	*std*	*med*	*max*	*mean*	*std*	*med*	*max*
Angle [deg]	6.13	4.24	5.94	17.30	3.45	2.62	2.91	9.22
Center [mm]	1.16	0.56	1.10	2.31	2.63	1.93	2.59	8.81
Size [mm]	2.63	1.56	2.36	6.72	1.28	0.94	1.21	3.33

Qualitative results and associated final NT measurements are in Fig. 4. Due to the space limitation, we only show 5 most accurate and 5 least accurate detection results along with the final NT region segmentations from 39 test results. The green and yellow boxes represent the ground truth poses of the fetal head and NT region, respectively. The red and cyan boxes correspond to the detected results. The following observations can be made from these results. As expected, the fetal head detection is very reliable because of its consistent appearance. Furthermore, the NT detection results are accurate for most cases, even for the 5 least accurate results. For most cases, the detected NT pose has lower accuracy in the horizontal direction along the NT edge. This is because of the ambiguity of the NT localization in this direction. However, the slight inaccuracy in the horizontal direction is less important for the segmentation and final NT measurement computation. The segmentation algorithm yields slightly better results of actual NT measurements for the 5 worst NT detection cases whose average error is 0.24 mm than for the 5 best NT detection results whose

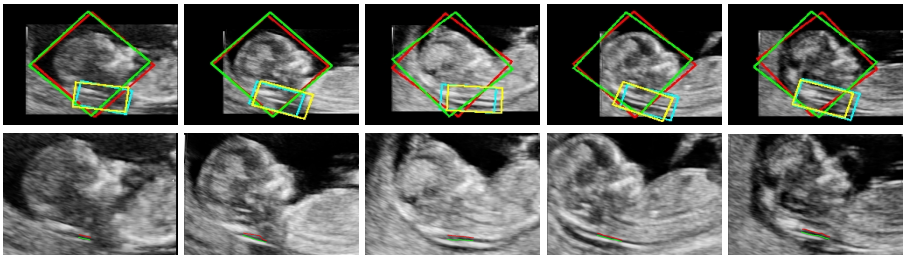

(a) Best detection examples of test data and their NT segmentation results.

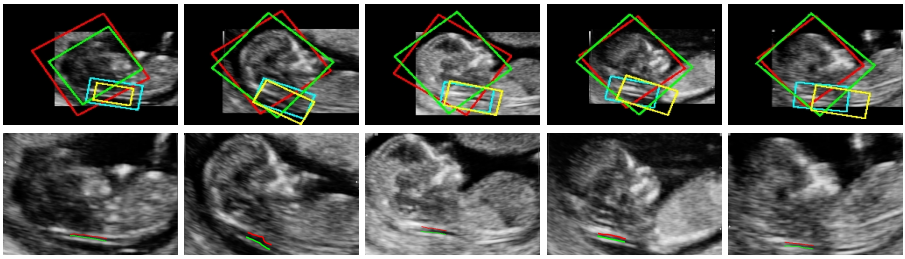

(b) Worst detection examples of test data and their NT segmentation results.

Fig. 4. Fetal head and NT detection results. The green and yellow boxes represent the ground truth poses of the fetal head and the NT region, respectively. The red and cyan box represent the fetal head and NT region detection results. The red and green lines highlight the upper and lower edge of the NT.

average error is 0.29 mm. It is evident that even when the NT detection box is less accurate, the NT measurement error is low and reliable.

6 Conclusion

This paper proposes a fully automatic approach for NT measurement. The algorithm starts by accurate detection of the fetal head pose. The fetal head serves as an anchoring structure and predicts the approximate pose of the NT region. The pose of the NT region is then locally refined and used to define a segmentation region. The initial edges of the NT region found by Dijkstra's shortest path are used to define seeds for accurate Graph Cut segmentation. Experimental results show that the proposed algorithm is robust and accurate. A slight inaccuracy in the detection of the NT location is caused by the ambiguity of the NT region localization along the edge of the neck but does not negatively impact the final measurement value.

The proposed algorithm can be extended to 3D ultrasound scans. To achieve this, mid-sagittal plane must be first found reliably. This can be done by relying on salient features inside the plane, but also by modeling fetal face profile after accurately detecting the fetal face [16]. This is an exciting direction of our future research and an important step towards automating routine measurements in obstetrics sonography.

References

1. Souka, A.P., Krampl, E., Bakalis, S., Heath, V., Nicolaides, K.H.: Outcome of pregnancy in chromosomally normal fetuses with increased nuchal translucency in the first trimester. Ultrasound in Obstetrics and Gynecology 18(1), 9–17 (2001)
2. Moratalla, J., Pintoffl, K., Minekawa, R., Lachmann, R., Wright, D., Nicolaides, K.H.: Semi-automated system for measurement of nuchal translucency thickness. Ultrasound in Obstetrics and Gynecology 36(4), 412–416 (2010)
3. Nirmala, S., Palanisamy, V.: Measurement of nuchal translucency thickness for detection of chromosomal abnormalities using first trimester ultrasound fetal images. Int'l J. of Computer Science and Information Security 6(3), 101–106 (2009)
4. Won, H.S., Hyun, M.K., Lee, H.: The clinical usefulness of volume NT using three-dimensional (3D) ultrasound. Samsung-Medison Article No. WP201012-VNT (2010)
5. Mortensen, E., Barrett, W.: Intelligent scissors for image composition. In: ACM Computer Graphics (SIGGRAPH), pp. 191–198 (1995)
6. Boykov, Y., Zabih, O.V., Fast, R.: approximate energy minimization via graph cuts. IEEE Trans. PAMI 23(11), 1222–1239 (2001)
7. Lu, W., Tan, J., Floyd, R.: Automated fetal head detection and measurement in ultrasound images by iterative randomized Hough transform. Ultrasound in Medicine & Biology 31(7), 929–936 (2005)
8. Chalana, V., Kim, Y.: A methodology for evaluation of boundary detection algorithms on medical images. IEEE Trans. Med. Imag. 16(5), 642–652 (1997)
9. Carneiro, G., Georgescu, B., Good, S., Comaniciu, D.: Detection and measurement of fetal anatomies from ultrasound images using a constrained probabilistic boosting tree. IEEE Trans. Med. Imag. 27(9), 1342–1355 (2008)
10. Tu, Z.: Probabilistic boosting-tree: Learning discriminative models for classification, recognition and clustering. In: Proc. of ICCV, pp. 1589–1596 (2005)
11. Deng, Y., Wang, Y., Chen, P., Yu, J.: A hierarchical model for automatic nuchal translucency detection. Computers in Biology and Medicine 42(6) (2012)
12. Zheng, Y., Barbu, A., Scheuering, M., Comaniciu, D.: Four-chamber heart modeling and automatic segmentation for 3D cardiac CT volumes using marginal space learning and steerable features. IEEE Trans. Med. Imag. 27(11), 1668–1681 (2008)
13. Zhang, J., Zhou, S., Comaniciu, D.: Joint real-time object detection and pose estimation using probabilistic boosting network. In: Proc. of CVPR (2007)
14. Sofka, M., Ralovich, K., Birkbeck, N., Zhang, J., Zhou, S.: Integrated detection network (idn) for pose and boundary estimation in medical images. In: ISBI (2011)
15. Sofka, M., Zhang, J., Zhou, S.K., Comaniciu, D.: Multiple object detection by sequential Monte Carlo and Hierarchical Detection Network. In: Proc. of CVPR (2010)
16. Feng, S., Zhou, S., Good, S., Comaniciu, D.: Automatic fetal face detection from ultrasound volumes via learning 3D and 2D information. In: Proc. of CVPR, pp. 2488–2495 (2009)